Published in final edited form as:
Sci Total Environ. 2020 November 20; 744: 140960. doi:10.1016/j.scitotenv.2020.140960.

Unexpected air quality impacts from implementation of green infrastructure in urban environments: A Kansas City case study

Yuqiang Zhang[a,h,*], **Jesse O. Bash**[b], **Shawn J. Roselle**[b], **Angie Shatas**[c], **Andrea Repinsky**[d], **Rohit Mathur**[b], **Christian Hogrefe**[b], **Jamie Piziali**[e], **Tom Jacobs**[f], **Alice Gilliland**[g]

[a]Oak Ridge Institute for Science and Education (ORISE) Fellowship Participant at U.S. Environmental Protection Agency, Research Triangle Park, NC 27711, United States of America

[b]Computational Exposure Division, National Exposure Research Laboratory, Office of Research and Development, U.S. Environmental Protection Agency, Research Triangle Park, NC 27711, United States of America

[c]Outreach Information Division, Office of Air Quality Planning and Standards, Office of Air and Radiation, U.S. Environmental Protection Agency, Research Triangle Park, NC 27711, United States of America

[d]Research Services Department, Mid-America Regional Council, Kansas City, MO 64105, United States of America

[e]Water Permits Division, Office of Wastewater Management, Office of Water, U.S. Environmental Protection Agency, Washington, DC 20460, United States of America

[f]Transportation and Environment, Mid-America Regional Council, Kansas City, MO 64105, United States of America

[g]National Risk Management Research Laboratory, Office of Research and Development, U.S. Environmental Protection Agency, Cincinnati, OH 45268, United States of America

[h]Nicholas School of the Environment, Duke University, Durham, NC 27708, United States of America

Abstract

[*]Corresponding author at: Nicholas School of the Environment, Duke University, 9 Circuit Dr, Durham, NC 27708, United States of America. Yuqiang.Zhang@duke.edu (Y. Zhang).

CRediT authorship contribution statement

Yuqiang Zhang: Conceptualization, Methodology, Formal analysis, Investigation, Data curation, Writing - original draft, Writing - review & editing, Visualization. **Jesse O. Bash:** Supervision, Methodology, Data curation, Resources, Writing - review & editing. **Shawn J. Roselle:** Supervision, Methodology, Resources. **Angie Shatas:** Resources. **Andrea Repinsky:** Resources. **Rohit Mathur:** Conceptualization, Methodology, Formal analysis, Investigation, Writing - review & editing. **Christian Hogrefe:** Conceptualization, Methodology, Formal analysis, Investigation, Writing - review & editing. **Jamie Piziali:** Resources. **Tom Jacobs:** Data curation. **Alice Gilliland:** Data curation.

Declaration of competing interest

The authors declare that they have no known competing financial interests or personal relationships that could have appeared to influence the work reported in this paper.

Appendix A. Supplementary data

Supplementary data to this article can be found online at https://doi.org/10.1016/j.scitotenv.2020.140960.

Green infrastructure (GI) implementation can benefit an urban environment by reducing the impacts of urban stormwater on aquatic ecosystems and human health. However, few studies have systematically analyzed the biophysical effects on regional meteorology and air quality that are triggered by changes in the urban vegetative coverage. In this study we use a state-of-the-art high-resolution air quality model to simulate the effects of a hypothetically feasible vegetation-focused GI implementation scenario in Kansas City, MO/KS on regional meteorology and air quality. Full year simulations are conducted for both the base case and GI land use scenarios using two different land surface models (LSMs) schemes inside the meteorological model. While the magnitudes of the changes in air quality due to the GI implementation differ using the two LSMs, the model outputs consistently showed increases in summertime $PM_{2.5}$ (1.1 μg m^{-3}, approximately 10% increase using NOAH LSM), which occurred mostly during the night and arose from the primary components, due to the cooler surface temperatures and the decreased planetary boundary layer height (PBLH). Both the maximum daily 8-hour average ozone and 1h daily maximum O_3 during summertime, decreased over the downtown areas (maximum decreases of 0.9 and 1.4 ppbv respectively). The largest ozone decreases were simulated to happen during the night, mainly caused by the titration effect of increased NO_x concentration from the lower PBLH. These results highlight the region-specific non-linear process feedback from GI on regional air quality, and further demonstrate the need for comprehensive coupled meteorological-air quality modeling systems and necessity of accurate land surface model for studying these impacts.

Graphical Abstract

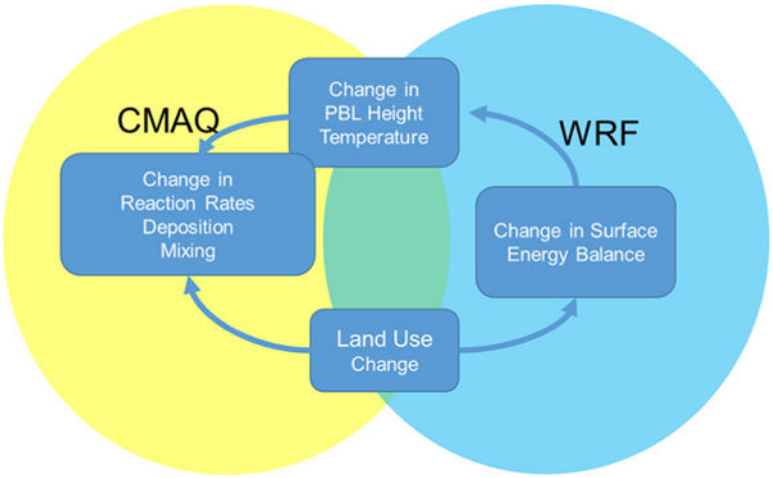

Keywords

Green infrastructure; Urban air quality; Temperature; Planetary boundary layer; Particular matter; Ozone

1. Introduction

The term ‘green infrastructure’ means the range of measures that use plant or soil systems, permeable pavement or other permeable surfaces or substrates, stormwater harvest and reuse, or landscaping to store, infiltrate, or evapotranspirate stormwater and reduce flows to

sewer systems or to surface waters. Green infrastructure (GI) implementation in urban areas can alleviate the impacts of urban stormwater on aquatic ecosystems and human health, improve the quality of both surface and ground water (Thomas, 2001; Brattebo and Booth, 2003; Davis et al., 2003; Ahn et al., 2005; Gilbert and Clausen, 2006; Zachary Bean et al., 2007; US EPA, 2009; Rowe, 2011), as well as significantly reduce surface air temperature (Gross, 2012; Santamouris, 2014; Žuvela-Aloise et al., 2016; Sharma et al., 2016), and therefore reduce energy consumption in air conditioning (Akbari et al., 2001; Donovan and Butry, 2009; He et al., 2015; Wang et al., 2018). The GI implementation could also cut the carbon dioxide levels, including direct effects of absorbing CO_2 though photolysis, and indirect effects of reducing CO_2 emission from power plants by reducing the cooling energy demand (Georgescu et al., 2014). Surface modification, such as increasing surface albedos and afforestation, could bring benefits of increases in the solar radiation reflected by Earth, and decreases in air temperature due to shade, the role of evaporation and transpiration in reducing sensible heat, and contribute to mitigating global climate change (Akbari et al., 2001; Zhang et al., 2016).

Previous studies have found benefits to air quality from GI implementations through the effects of vegetation cover changes on pollutant dispersion and deposition (Currie and Bass, 2008; Nowak et al., 2006, 2013, 2014, 2018; Tallis et al., 2011; Pugh et al., 2012; Wu et al., 2012; Irga et al., 2015; Jeanjean et al., 2016; Selmi et al., 2016; Abhijith et al., 2017; Jayasooriya et al., 2017; Yli-Pelkonen et al., 2017a, 2017b; Sicard et al., 2018). However, few studies have considered the dynamic and chemical changes associated with increased urban vegetation cover. Urban vegetation reduces surface temperatures, which in turn reduces chemical reaction rates, especially for secondary air pollutants, such as ozone (O_3) and secondary organic aerosols (SOA). Cooling temperatures also decrease biogenic hydrocarbon emissions (Fu et al., 2014; Ghirardo et al., 2016), which are also important precursors for O_3 and fine particulate matter ($PM_{2.5}$). A recent study that utilized a coupled meteorological and chemistry model predicted that an increase of surface albedo could decrease surface temperatures and the planetary boundary layer height (PBLH), but this effect resulted in a negligible decrease in both 8-hour average ozone concentrations and 24-hour averaged $PM_{2.5}$ during a three-day long heatwave episode in Montreal, Canada (Touchaei et al., 2016). The reduced PBLH from cooler temperatures could also increase air pollutant concentrations (Long et al., 2018), especially for the primary gaseous pollutants (i.e., nitric oxides; NO_X) that are important precursors for O_3 production, as well as for primary (locally emitted) particulate pollutants (i.e., primary nitrates, sulfates and ammonium). Meanwhile, temperature changes could also affect cloud cover and precipitation, which can affect the deposition of air pollutants.

Because of the competing factors and non-linear interactions of these processes, assessment of the potential impacts of increased vegetative cover and/or surface albedo requires the use of full prognostic meteorological and photochemical models (Taha, 2008a, 2008b, 2008c). In this study, we use a state-of-the-art coupled meteorological-chemistry model (Weather Research and Forecasting - Community Multi-scale Air Quality a.k.a., WRF-CMAQ; Wong et al., 2012) with the Noah land surface model (Noah LSM, Campbell et al., 2019) to simulate the effect of solely increasing vegetation in Kansas City (KC), MO/KS on regional meteorology and air quality. The GI scenario used in this study was provided by the Mid-

America Regional Council (MARC), and included modifications to land cover data consistent with widespread adoption of GI projects, such as urban reforestation and wetland restoration, as in Fig. 1. The major land use categories changes between the hypothetical GI and current scenario can be seen in Fig. S4.

2. Materials and methods

2.1. The coupled WRF-CMAQ model configurations

Air quality simulations were performed using the CMAQ version 5.2 on a domain covering the contiguous U.S. with 12-km horizontal resolution and inner domain with 4-km horizontal resolution and 35 vertical layers (see Fig. S1). Gas-phase chemistry was simulated with revision 3 of the Carbon Bond 2006 mechanism (CB6r3), inorganic aerosol thermodynamics were based on ISORROPIA II (Nenes et al., 1998, 1999), an extendable aqueous phase chemistry option (AQCHEM – KMT, Fahey et al., 2017), primary organic aerosol was modeled as non-volatile, and secondary organic aerosol was based on Pye et al. (2017). Boundary conditions were developed from a CMAQ simulation on a larger domain that used boundary conditions based on a hemispheric CMAQ simulation (Mathur et al., 2017). U.S. anthropogenic emissions were based primarily on version 4 of the 2011 national emission inventory (last accessed March 3, 2019). Emissions representative of 2011 for biogenic compounds (Rasool et al., 2016), windblown dust (Foroutan et al., 2017) and lightning NO emissions (Allen and Pickering, 2002) are simulated inline, and NH_3 surface-exchange was simulated with CMAQ using a bidirectional exchange parameterization (Bash et al., 2013; Pleim et al., 2013). Meteorological fields for CMAQ modeling were based on coupled WRF (v3.8.1) model. Physics options for the WRF included the asymmetric convective model version 2 planetary boundary layer (Pleim, 2007), the Kain-Fritsch convective cumulus parameterization (Kain, 2004) with lightning assimilation (Heath et al., 2016), and the Morrison two-moment microphysics scheme (Morrison et al., 2008). We used two different land surface model (LSM), Noah (Chen and Dudhia, 2001; Campbell et al., 2019) and Pleim-Xiu land-surface model (Pleim and Xiu, 2003). The default and most widely used LSM inside the coupled WRF-CMAQ model is Pleim-Xiu (PX). Results are focused on the Noah LSM results because the PX LSM constrains the surface fluxes by continuously adjusting soil moisture and temperature to minimize model errors in 2 m temperature and mixing ratio, compared with observed surface analyses with nudging coefficients based on model parameters such as solar radiation, temperature, leaf area, vegetation coverage, and aerodynamic resistance (Pleim and Gilliam, 2009). After the nudging processes, we found the WRF-PX LSM dampened the feedbacks from vegetation cover changes on the regional temperature.

2.2. Model evaluation

A full year simulation in 2011 was carried out in our study at both 12 km and 4 km resolution. We evaluated the model's performance in simulating $PM_{2.5}$ and O_3 during both summer and winter time by comparing with observations in JJA (June–July–August) and DJF (December–January–February) at Air Quality System (AQS) datasets (Supporting Fig. S1). Here we focused on Kansas City only, since the coupled model performance over the U.S. has been recently comprehensively evaluated (Wong et al., 2012; Appel et al., 2017). In

summertime, the mean $PM_{2.5}$ concentration in Kansas City is 11.1 μg m^{-3} from the AQS observation sites, while the mean from the coupled WRF-CMAQ model is 9.3 μg m^{-3}. The coupled WRF-CMAQ model underestimates the summertime $PM_{2.5}$ concentration in Kansas City with MB (mean bias) of −1.78 μg m^{-3}, and NMB (normalized mean bias) of −16.1% (Fig. S2a). During wintertime, the coupled WRF-CMAQ overestimates $PM_{2.5}$ (MB of 3.4 μg m^{-3}, and NMB of 27.6%), compared with the AQS sites (Fig. S2d). During summertime the mean MDA8 O_3 from the observations in Kansas City is 53.5 ppbv, and 60.6 ppbv from the coupled model. The coupled WRF-CMAQ model overestimated the MDA8 O_3 with MB of 7.24 ppbv and NMB of 13.6% (Fig. S2b). During wintertime, however, the coupled WRF-CMAQ model underestimates the MDA8 O_3 (MB of −3.10 ppbv and NMB of −10.6%, Fig. S2e). We observed similar patterns for 1 h daily maximum ozone with the MDA8 O_3, overestimating during summertime and underestimating during wintertime (Fig. S2c, f). We also evaluated WRF's performance by comparing the summertime daily maximum temperature, daily minimum temperature and the daily mean temperature for the 8 counties in Kansas city (Table S1), downloaded from the Midwestern Regional Climate Center (https://mrcc.illinois.edu/CLIMATE/welcome.jsp, accessed Feb 05, 2020). In general, the WRF model has a satisfying performance in predicting the summertime temperature in the Kansas city, with slightly overestimating compared with observation (Fig. S3). However, notice that the bias in the evaluation does not necessarily lead to bias in estimated changes induced by green infrastructure changes.

2.3. The GI scenario design by MARC

The Mid-America Regional Council, the association of city and county governments for the bi-state Kansas City region, created 2.5 m land cover data using 2012 SPOT imagery. The land use and land cover data generated by MARC were then mapped to NLCD land use categories used in the WRF-CMAQ modeling system and in the estimation of biogenic volatile carbon emissions. Table S2 details the MARC land use classification scheme and the mapping to the NLCD land use categories used by WRF and CMAQ in these model simulations.

A feasible vegetative focused green infrastructure scenario was developed for Kansas City by applying the following changes to the base land cover data:

1. Change impervious or cultivated cover to forest cover within 150′ of streams. This assumes restoration of riparian forest occurs within buffers of all streams;
2. Change herbaceous cover to forest outside of 50 ft buffer of arterials, within activity centers. MARC mapped activity centers, or areas of concentration of employment and non-residential activity, by a). select non-residential building footprints, b). create a density raster of the building footprint centroids, c). create a density raster of the building footprint centroids, weighted by the area of the building footprints, and d). combine both rasters into one index of centerness. The original land cover data shows that most commercial areas and other activity centers in the region contain very few trees. This step assumes widespread planting of trees within activity centers as a replacement of urban turf.
3. Split 'impervious other' class into road impervious vs. parking impervious.

4. Change impervious other to shrub-scrub cover outside of 50 ft buffer of arterials, within activity centers. First, MARC isolated parking areas from the generalized non-building impervious class. Then, MARC selected shrub-scrub cover to fill parking areas within activity centers as a way to assume that parking lots remain, but that they are retrofitted with vegetated islands. Shrub-scrub cover is defined by shrubs and trees covering 10–50% of the ground, which is consistent with this assumption.
5. Change freeway and interstate right-of-way, and herbaceous cover within parks, golf courses, and cemeteries, from herbaceous cover to a new grassland cover class. This step assumes that turf cover in highway rights-of-way and turf within other public and semi-public land will be restored to native tallgrass prairie species.
6. Change a 50 ft buffer of arterials to shrub-scrub cover, assuming widespread planting of street trees.
7. Change cultivated areas in floodplain to lowland herbaceous/cultivated cover. This step assumes that some of the areas that had been converted from wetlands to agricultural use would be restored as wetlands.

The same mapping was applied to the GI scenario as the base scenario (Table S2). This updated land use data then replaced the NLCD data distributed with WRF version 3.8.1 and in the Biogenic Emissions Land use Database (BELD) data used to estimate biogenic volatile organic compound emissions (Bash et al., 2016). Updated land use data was written to the WRF input file and BELD and then propagated into the WRF-CMAQ modeling system.

3. Results and discussion

In the GI scenario provided by MARC for KC, there are increases in the vegetated natural areas, and decreases in agricultural and urban areas. Developed areas, including open space, and low, medium and high intensity classifications in the KC downtown areas, have been transformed into forest, herbaceous and shrubland areas (Fig. S4, Table S2). Under the GI scenario, there is also a switch from cultivated crops to wetlands (including woody wetlands and emergent herbaceous wetlands; Figs. S4e, f, S5 and Table S2) over the river basins. The leaf area index (LAI) and vegetation fraction are projected to increase across the city (Fig. 2), especially during the summertime (Figs. S6–S7), except on the northeast of the domain over the Missouri River basins where the cultivated crops usually have larger LAI than that from emergent herbaceous wetlands, especially during the growing seasons.

Although annual simulations were performed, our discussion focuses on summertime when conditions are more favorable for ozone formation. The main results for other seasons can also be seen in the Supporting materials. In the following sections, we will discuss the meteorological and air quality changes in summer induced from the vegetation cover changes from the GI implementation in the KC area.

3.1. GI implementation impacts on meteorology

Changes in vegetation fraction affects the energy balance between latent heat flux and sensible heat flux which in turn affects surface temperatures. Larger changes are seen during the summer season (June–July-August; JJA) than in other seasons for both the 2-m surface temperature (T2) and PBLH (Figs. S8–S9). Fig. 3 shows that T2 decreases throughout the KC area as a result of increases in the latent heat flux and decreases of sensible heat flux (Fig. S10): here, the increased vegetative fraction repartitions the energy from sensible heat flux to the latent heat flux, which cools down the surface. The change of surface albedo could also contribute to the surface cooling which was not shown here. The 2-m surface temperature is reduced over urban areas by more than 0.3 °C, especially over the KC downtown areas, with a maximum decrease of 0.7 °C. For the diurnal T2 change, the largest T2 decreases occur during the daytime (Fig. S11a, b), because of the strong evapotranspiration effects from the increased vegetation. There are also increases in T2 over the northern and southern portion of the domain, resulting from repatriating the energy from latent heat flux to the sensible heat flux (Fig. S10), which warm the surface due to LAI changes as a result of switches from cultivated crops to wetlands (Fig. S4). The JJA PBLH differences have similar patterns to T2, with the most significant decreases (90 m) over the downtown KC, and increases in PBLH (largest increase of 81 m) over the northern and southern KC area. The PBLH changes are also larger during the daytime than that in the nighttime, following the T2 diurnal change patterns (Fig. S11c, d).

3.2. GI implementation impacts on surface air quality

For both the base and GI simulations, the configurations are the same, except for the land use changes. The air quality changes from these two simulations are due to the land use induced chemical and physical processes. Fig. 4 shows the changes in the 24-hour average, daytime (from 9 am to 7 pm local time in KC), and nighttime $PM_{2.5}$ during JJA. We can see that the three-month averaged $PM_{2.5}$ concentrations increased throughout most of the domain, especially over the downtown areas, with a maximum increase of 1.1 μg m^{-3} (10%). Most of the $PM_{2.5}$ increases occur at night when the PBL shrinks. The increased vegetative cover in the GI scenario causes the nighttime PBLH to be lower than the base, increasing the pollutant concentrations, as this decreased volume restricts the ventilation of pollutants. $PM_{2.5}$ concentrations also decrease during the daytime (Fig. S12), especially at the northern and southern portions of the domain (Fig. 4b), likely caused by the slower chemical reaction rates from the relatively lower temperatures in the GI scenario. The PBLH also increases over these same areas during the daytime, decreasing $PM_{2.5}$ concentrations. These increases are mainly caused by changes in the primary components of $PM_{2.5}$, such as elementary carbon (EC, Fig. 5e), unspeciated components (UNSPEC1, Fig. 5f), and primary organic carbon (POC, Fig. S13), which are more sensitive to the lower PBL changes.

The summertime maximum daily 8-hour average ozone (MDA8 O_3), as well as 1-hour daily maximum O_3 (1hrMax O_3), are projected to decrease over the downtown areas (the maximum decreases are 0.9 and 1.4 ppbv for MDA8 O_3 and 1hrMax O_3, respectively), but increase over the northern and southern portions of the domain (Fig. 6b, c), following similar patterns as the T2 changes (Fig. 2a). The 24-hour average O_3 has larger decreases than the MDA8 O_3 and 1hrMax O_3 (Fig. 6a). When separating the surface ozone changes into

daytime and nighttime, we find that the JJA averaged ozone has larger decreases during the night (reaching 5.2 ppbv over the downtown regions, Fig. S14). This is likely caused by the increased NO_x titration effects on O_3 during the night from the lowered PBLH (Fig. S15). The decreased PBLH increases NO_x concentrations by up to 12ppbv during the night over the downtown regions (Fig. S14b). Maximum O_3 decreases over the downtown are influenced by increased O_3 dry deposition from increased vegetation fraction (Fig. S16) and possibly slower chemical reaction rates from reduced air temperatures (Fig. 3a). Unlike $PM_{2.5}$, the decreasing PBLH over the downtown area does not dominate surface ozone changes over the urban areas in KC. Instead the decreasing PBLH increased the NO_x concentration which decreases the ozone concentration by increasing the NO_x titration effect. From the mean JJA diurnal O_3 changes over the KC region, the surface O_3 significantly decreases in the night and early morning (Fig. S17). The domain average of JJA O_3 changes in KC are 0.3 ppbv.

3.3. Sensitivity analysis using different land surface model

For this study, we also perform another set of sensitivity simulations using the Pleim-Xiu land surface model (PX LSM, see methods) inside the WRF-CMAQ. The PX LSM is widely used in retrospective air quality studies (Hogrefe et al., 2015; Ran et al., 2016), and is being used here to test the robustness of our study results. One note concerning the PX LSM is that it is constrained by surface moisture and temperature with observations, which could dampen the signals from the land use changes. From Fig. 7, we see that the T2 and PBLH changes using the PX LSM have similar patterns as those using the Noah LSM (Fig. 3), except that the magnitudes of the changes are relatively smaller. The maximum decrease for the JJA T2 is 0.3 °C (compared with 0.7 °C for the Noah LSM), and 61 m for JJA PBLH (compared to 90 m for the Noah LSM). The mean JJA air quality changes are also smaller compared to the simulation that used the Noah LSM, with maximum increases of 0.6 μg m^{-3} for surface $PM_{2.5}$, and maximum decrease of 1.4 ppbv for 24-h O_3.

This study uses a state-of-the-art regional air quality model to investigate the effects of a possible green infrastructure (GI) scenario on regional meteorology and air quality in Kansas City (KC). Vegetative fractions and leaf area indexes increase in the GI scenario, especially over the KC downtown area, as developed areas are replaced with more vegetated natural areas. The impervious surfaces also decrease in accordance with the land use type transition. The regional temperature and planetary boundary height (PBLH) over this area are projected to decrease as the evapotranspiration from increased vegetation reduces sensible heat fluxes. The surface ozone concentrations are projected to decrease as much as 2.0 ppbv during the daytime, and 5.2 ppbv during the nighttime. The JJA daytime O_3 decreases reflect the competing effects from increased ozone dry deposition and slower chemical reaction rates, while the much larger ozone decrease noted during the nighttime is due to NO_x titration effects attributable to the lower PBLH. The increased vegetation cover also affects surface $PM_{2.5;}$ summertime $PM_{2.5}$ concentrations over the KC downtown area are projected to increase as high as 10% (about 1.1 μg m^{-3}), especially during the night. The lower PBLH is responsible for the $PM_{2.5}$ concentration increases, especially for the primary $PM_{2.5}$ components (i.e., elementary carbon, primary organic carbon and unspeciated portion of $PM_{2.5}$ emissions).

When referring to the conclusions, we should keep in mind that these results are for a specific GI scenario which was developed as part of a storm water management plan for the urban area of KC, and not as a plan for urban heat island mitigation. The results may vary depending on the GI scenario introduced, as well as the topography of the region. In particular, electricity generating units emissions change to account for changes in electricity demand due to changes in air temperatures. Biogenic emissions may increase due to additional biomass in the region but may decrease regionally due to lower temperatures, which are not quantified in this study. The results from this study can inform other similar studies, such as examining the impact of urban heat island mitigation strategies (e.g., green roofs/white roofs). This study indicates air quality changes in O_3 and $PM_{2.5}$ associated with the additional shading and vegetation transpiration effects from an aggressive GI implementation scenario may have confounding ecologic and economic benefits from such as a strategy. Additional research is needed to understand these effects on anthropogenic and biogenic emissions to fully capture air quality impacts, which would be especially important for areas exceeding the $PM_{2.5}$ National Ambient Air Quality Standard. Other meteorological effects, such as changes in wind direction, wind speed, the relative humidity, surface moisture, terrestrial erosion, and surface roughness, which could also directly or indirectly influence the air quality. Further follow-up research should consider to develop algorithms to quantify the relative contribution of these effects.

Supplementary Material

Refer to Web version on PubMed Central for supplementary material.

Acknowledgment

This research was supported in part by an appointment to the Research Participation Program at the U.S. Environmental Protection Agency (EPA), Office of Research and Development, administered by the Oak Ridge Institute for Science and Education (ORISE) through an interagency agreement between the U.S. Department of Energy and the U.S. EPA. We would like to thank Kirk Baker and Val Garcia from U.S. EPA for their insightful suggestions for improving the initial version of this manuscript. The views expressed in this article are those of the authors and do not necessarily reflect the views or policies of the U.S. EPA.

References

Abhijith KV, Kumar P, Gallagher J, McNabola A, Baldauf R, Pilla F, Broderick B, Di Sabatino S, Pulvirenti B, 2017 Air pollution abatement performances of green infrastructure in open road and built-up street canyon environments – a review. Atmos. Environ 162, 71–86. 10.1016/j.atmosenv.2017.05.014.

Ahn JH, Grant SB, Surbeck CQ, Digiacomo PM, Nezlin NP, Jiang S, 2005 Coastal water quality impact of stormwater runoff from an urban watershed in Southern California. Environ. Sci. Technol 39, 5940–5953. 10.1021/es0501464. [PubMed: 16173550]

Akbari H, Pomerantz M, Taha H, 2001 Cool surfaces and shade trees to reduce energy use and improve air quality in urban areas. Sol. Energy 70, 295–310. 10.1016/S0038-092X(00)00089-X.

Allen DJ, Pickering KE, 2002 Evaluation of lightning flash rate parameterizations for use in a global chemical transport model. J. Geophys. Res. Atmos 107, 1–21. 10.1029/2002JD002066.

Appel KW, Napelenok SL, Foley KM, Pye HOT, Foley KM, Spero TL, Appel KW, Pleim JE, Gilliam RC, Fahey KM, Kang D, Luecken DJ, Pouliot GA, Wong DC, Roselle SJ, Foroutan H, Sarwar G, Napelenok SL, Young JO, Bash JO, Hutzell WT, Hogrefe C, Heath NK, Mathur R, Schwede DB, Gantt B, 2017 Description and evaluation of the Community Multiscale Air Quality (CMAQ)

modeling system version 5.1. Geosci. Model Dev 10, 1703–1732. 10.5194/gmd-10-1703-2017. [PubMed: 30147852]

Bash JO, Cooter EJ, Dennis RL, Walker JT, Pleim JE, 2013 Evaluation of a regional air-quality model with bidirectional NH3 exchange coupled to an agroecosystem model. Biogeosciences 10, 1635–1645. 10.5194/bg-10-1635-2013.

Bash JO, Baker KR, Beaver MR, 2016 Evaluation of improved land use and canopy representation in BEIS v3.61 with biogenic VOC measurements in California. Geosci. Model Dev 9, 2191–2207. 10.5194/gmd-9-2191-2016.

Brattebo BO, Booth DB, 2003 Long-term stormwater quantity and quality performance of permeable pavement systems. Water Res. 37, 4369–4376. 10.1016/S0043-1354(03)00410-X. [PubMed: 14511707]

Campbell PC, Bash JO, Spero TL, 2019 Updates to the Noah Land Surface Model in WRF-CMAQ to improve simulated meteorology, air quality, and deposition. J. Adv. Model. Earth Syst 10.1029/2018MS001422.

Chen F, Dudhia J, 2001 Coupling an advanced land surface–hydrology model with the Penn State–NCAR MM5 modeling system. Part I: model implementation and sensitivity. Mon. Weather Rev 129, 569–585. 10.1175/1520-0493(2001) 129b0569:CAALSHN2.0.CO;2.

Currie BA, Bass B, 2008 Estimates of air pollution mitigation with green plants and green roofs using the UFORE model. Urban Ecosyst. 11, 409–422. 10.1007/s11252-008-0054-y.

Davis AP, Shokouhian M, Sharma H, Minami C, Winogradoff D, 2003 Water quality improvement through bioretention: lead, copper, and zinc removal. Water Environ. Res 75, 73–82. 10.2175/106143003X140854. [PubMed: 12683466]

Donovan GH, Butry DT, 2009 The value of shade: estimating the effect of urban trees on summertime electricity use. Energy Build 41, 662–668. 10.1016/j.enbuild.2009.01.002.

Fahey KM, Carlton AG, Pye HOT, Baek J, Hutzell WT, Stanier CO, Baker KR, Wyat Appel K, Jaoui M, Offenberg JH, 2017 A framework for expanding aqueous chemistry in the Community Multiscale Air Quality (CMAQ) model version 5.1. Geosci. Model Dev 10, 1587–1605. 10.5194/gmd-10-1587-2017. [PubMed: 30147851]

Foroutan H, Young JO, Napelenok SL, Ran L, Appel KW, Gilliam RC, Pleim JE, 2017 Development and evaluation of a physics-based windblown dust emission scheme implemented in the CMAQ modeling system. J. Adv. Model. Earth Syst 9, 1248–1269. 10.1002/2016MS000823.

Fu Y, Liao H, Change C, 2014 Impacts of land use and land cover changes on biogenic emissions of volatile organic compounds in China from the late 1980s to the mid- 2000s: implications for tropospheric ozone and secondary organic aerosol. Tellus B 66, 1–17. 10.3402/tellusb.v66.24987.

Georgescu M, Morefield PE, Bierwagen BG, Weaver CP, 2014 Urban adaptation can roll back warming of emerging megapolitan regions. Proc. Natl. Acad. Sci 111, 2909–2914. 10.1073/pnas.1322280111. [PubMed: 24516126]

Ghirardo A, Xie J, Zheng X, Wang Y, Grote R, Block K, Wildt J, Mentel T, Kiendler-Scharr A, Hallquist M, Butterbach-Bahl K, Schnitzler JP, 2016 Urban stress-induced biogenic VOC emissions and SOA-forming potentials in Beijing. Atmos. Chem. Phys 16, 2901–2920. 10.5194/acp-16-2901-2016.

Gilbert JK, Clausen JC, 2006 Stormwater runoff quality and quantity from asphalt, paver, and crushed stone driveways in Connecticut. Water Res. 40, 826–832. 10.1016/j.watres.2005.12.006. [PubMed: 16427680]

Gross G, 2012 Effects of different vegetation on temperature in an urban building environment. Micro-scale numerical experiments. Meteorol. Zeitschrift 21, 399–412. 10.1127/0941-2948/2012/0363.

He Y, Yu H, Zhao M, 2015 Thermal performance study of extensive green roof in Shanghai District: a case study of lightweight building in winter. Procedia Eng 121, 1597–1604. 10.1016/j.proeng.2015.09.186.

Heath NK, Pleim JE, Gilliam RC, Kang D, 2016 A simple lightning assimilation technique for improving retrospective WRF simulations. J. Adv. Model. Earth Syst 8, 1248–1269. 10.1002/2016MS000689.

Hogrefe C, Pouliot G, Wong D, Torian A, Roselle S, Pleim J, Mathur R, 2015 Annual application and evaluation of the online coupled WRF-CMAQ system over North America under AQMEII phase 2. Atmos. Environ 115, 683–694. 10.1016/j.atmosenv.2014.12.034.

Irga PJ, Burchett MD, Torpy FR, 2015 Does urban forestry have a quantitative effect on ambient air quality in an urban environment? Atmos. Environ 120, 173–181. 10.1016/j.atmosenv.2015.08.050.

Jayasooriya VM, Ng AWM, Muthukumaran S, Perera BJC, 2017 Green infrastructure practices for improvement of urban air quality. Urban For. Urban Green 21, 34–47. 10.1016/j.ufug.2016.11.007.

Jeanjean APR, Monks PS, Leigh RJ, 2016 Modelling the effectiveness of urban trees and grass on PM2.5reduction via dispersion and deposition at a city scale. Atmos. Environ 147, 1–10. 10.1016/j.atmosenv.2016.09.033.

Kain JS, 2004 The Kain–Fritsch convective parameterization: an update. J. Appl. Meteorol 43, 170–181. 10.1175/1520-0450(2004)043b0170:TKCPAUN2.0.CO;2.

Long X, Wu J, Li X, Feng T, Xing L, Zhao S, Cao J, Tie X, An Z, Li G, Bei N, 2018 Does afforestation deteriorate haze pollution in Beijing-Tianjin-Hebei (BTH), China? Atmos. Chem. Phys 18, 10869–10879. 10.5194/acp-18-10869-2018.

Mathur R, Xing J, Gilliam R, Sarwar G, Hogrefe C, Pleim J, Pouliot G, Roselle S, Spero TL, Wong DC, Young J, 2017 Extending the Community Multiscale Air Quality (CMAQ) modeling system to hemispheric scales: overview of process considerations and initial applications. Atmos. Chem. Phys 17, 12449–12474. 10.5194/acp-17-12449-2017. [PubMed: 29681922]

Morrison H, Thompson G, Tatarskii V, 2008 Impact of cloud microphysics on the development of trailing stratiform precipitation in a simulated squall line: comparison of one- and two-moment schemes. Mon. Weather Rev 137, 991–1007. 10.1175/2008mwr2556.1.

Nenes A, Pandis SN, Pilinis C, 1999 Continued development and testing of a new thermodynamic aerosol module for urban and regional air quality models. Atmos. Environ 33, 1553–1560. 10.1016/S1352-2310(98)00352-5.

Nowak DJ, Crane DE, Stevens JC, 2006 Air pollution removal by urban trees and shrubs in the United States. Urban For. Urban Green 4, 115–123. 10.1016/j.ufug.2006.01.007.

Nowak DJ, Hirabayashi S, Bodine A, Hoehn R, 2013 Modeled PM2.5 removal by trees in ten U.S. cities and associated health effects. Environ. Pollut 178, 395–402. 10.1016/j.envpol.2013.03.050. [PubMed: 23624337]

Nowak DJ, Hirabayashi S, Bodine A, Greenfield E, 2014 Tree and forest effects on air quality and human health in the United States. Environ. Pollut 193, 119–129. 10.1016/j.envpol.2014.05.028. [PubMed: 25016465]

Nowak DJ, Hirabayashi S, Doyle M, McGovern M, Pasher J, 2018 Air pollution removal by urban forests in Canada and its effect on air quality and human health. Urban For. Urban Green 29, 40–48. 10.1016/j.ufug.2017.10.019.

Pleim JE, 2007 A combined local and nonlocal closure model for the atmospheric boundary layer. Part I: model description and testing. J. Appl. Meteorol. Climatol 46, 1383–1395. 10.1175/jam2539.1.

Pleim JE, Gilliam R, 2009 An indirect data assimilation scheme for deep soil temperature in the Pleim-Xiu land surface model. J. Appl. Meteorol. Climatol 48, 1362–1376. 10.1175/2009JAMC2053.1.

Pleim JE, Xiu A, 2003 Development of a land surface model. Part II: data assimilation. J. Appl. Meteorol 42, 1811–1822. 10.1175/1520-0450(2003) 042b1811:doalsmN2.0.co;2.

Pleim JE, Bash EO, Walker JT, Cooter EJ, 2013 Development and evaluation of an ammonia bidirectional flux parameterization for air quality models. J. Geophys. Res. Atmos 118, 3794–3806. 10.1002/jgrd.502622013.

Pugh TAM, MacKenzie AR, Whyatt JD, Hewitt CN, 2012 Effectiveness of green infrastructure for improvement of air quality in urban street canyons. Environ. Sci. Technol 46, 7692–7699. 10.1021/es300826w. [PubMed: 22663154]

Pye HOT, Murphy BN, Xu L, Ng NL, Carlton AG, Guo H, Weber R, Vasilakos P, Wyat Appel K, Hapsari Budisulistiorini S, Surratt JD, Nenes A, Hu W, Jimenez JL, Isaacman-Vanwertz G, Misztal PK, Goldstein AH, 2017 On the implications of aerosol liquid water and phase separation for organic aerosol mass. Atmos. Chem. Phys 17, 343–369. 10.5194/acp-17-343-2017. [PubMed: 30147709]

Ran L, Pleim J, Gilliam R, Binkowski FS, Hogrefe C, Band L, 2016 Improved meteorology from an updated WRF/CMAQ modeling system with MODIS vegetation and albedo. J. Geophys. Res. Atmos. Res 121, 2393–2415. 10.1002/2015JD024406.

Rasool QZ, Zhang R, Lash B, Cohan DS, Cooter EJ, Bash JO, Lamsal LN, 2016 Enhanced representation of soil NO emissions in the Community Multiscale Air Quality (CMAQ) model version 5.0.2. Geosci. Model Dev 9, 3177–3197. 10.5194/gmd-9-3177-2016.

Rowe DB, 2011 Green roofs as a means of pollution abatement. Environ. Pollut 159, 2100–2110. 10.1016/j.envpol.2010.10.029. [PubMed: 21074914]

Santamouris M, 2014 Cooling the cities - a review of reflective and green roof mitigation technologies to fight heat island and improve comfort in urban environments. Sol. Energy 103, 682–703. 10.1016/j.solener.2012.07.003.

Selmi W, Weber C, Rivière E, Blond N, Mehdi L, Nowak D, 2016 Air pollution removal by trees in public green spaces in Strasbourg city, France. Urban For. Urban Green 17, 192–201. 10.1016/j.ufug.2016.04.010.

Sharma A, Conry HJS, Hamket AF, Hellmann JJ, Chen F, 2016 Green and cool roofs to mitigate urban heat island effect in the Chicago metropolitan evaluation with a regional climate model. Environ. Res. Lett 11, 1–15. 10.1088/1748-9326/11/6/064004.

Sicard P, Agathokleous E, Araminiene V, Carrari E, Hoshika Y, De Marco A, Paoletti E, 2018 Should we see urban trees as effective solutions to reduce increasing ozone levels in cities? Environ. Pollut 243, 163–176. 10.1016/j.envpol.2018.08.049. [PubMed: 30172122]

Taha H, 2008a Episodic performance and sensitivity of the urbanized MM5 (uMM5) to perturbations in surface properties in Houston Texas. Boundary-Layer Meteorol 127, 193–218. 10.1007/s10546-007-9258-6.

Taha H, 2008b Meso-urban meteorological and photochemical modeling of heat island mitigation. Atmos. Environ 42, 8795–8809. 10.1016/j.atmosenv.2008.06.036.

Taha H, 2008c Urban surface modification as a potential ozone air-quality improvement strategy in California: a mesoscale modelling study. Boundary-Layer Meteorol 127, 219–239. 10.1007/s10546-007-9259-5.

Tallis M, Taylor G, Sinnett D, Freer-Smith P, 2011 Estimating the removal of atmospheric particulate pollution by the urban tree canopy of London, under current and future environments. Landsc. Urban Plan 103, 129–138. 10.1016/j.landurbplan.2011.07.003.

Thomas MA, 2001 The effect of residential development on ground-water quality near Detroit, Michigan. J. Am. Water Resour. Assoc 36, 1023–1038.

Touchaei AG, Akbari H, Tessum CW, 2016 Effect of increasing urban albedo on meteorology and air quality of Montreal (Canada) - episodic simulation of heat wave in 2005. Atmos. Environ 132, 188–206. 10.1016/j.atmosenv.2016.02.033.

US EPA, 2009 Green Roofs for Stormwater Runoff Control (PDF). Publication No. EPA/600/R-09/026|Abstract. U. S. Environmental Protection Agency, Washington, DC.

Wang C, Wang ZH, Yang J, 2018 Cooling effect of urban trees on the built environment of contiguous United States. Earth's Futur 6, 1066–1081. 10.1029/2018EF000891.

Wong DC, Pleim J, Mathur R, Binkowski F, Otte T, Gilliam R, Pouliot G, Xiu A, Young JO, Kang D, 2012 WRF-CMAQ two-way coupled system with aerosol feedback: software development and preliminary results. Geosci. Model Dev 5, 299–312. 10.5194/gmd-5-299-2012.

Wu S, Mickley LJ, Kaplan JO, Jacob DJ, 2012 Impacts of changes in land use and land cover on atmospheric chemistry and air quality over the 21st century. Atmos. Chem. Phys 12, 1597–1609. 10.5194/acp-12-1597-2012.

Yli-Pelkonen V, Scott AA, Viippola V, Setälä H, 2017a Trees in urban parks and forests reduce O_3, but not NO_2 concentrations in Baltimore, MD, USA. Atmos. Environ 167, 73–80. 10.1016/j.atmosenv.2017.08.020.

Yli-Pelkonen V, Setälä H, Viippola V, 2017b Urban forests near roads do not reduce gaseous air pollutant concentrations but have an impact on particles levels. Landsc. Urban Plan 158, 39–47. 10.1016/j.landurbplan.2016.09.014.

Zachary Bean E, Frederick Hunt W, Alan Bidelspach D, 2007 Evaluation of four permeable pavement sites in eastern North Carolina for runoff reduction and water quality impacts. J. Irrig. Drain. Eng 133, 583–592. 10.1061/(ASCE)0733-9437(2007)133:6(583).

Zhang J, Zhang K, Liu J, Ban-Weiss G, 2016 Revisiting the climate impacts of cool roofs around the globe using an Earth system model. Environ. Res. Lett 11, 1–11. 10.1088/1748-9326/11/8/084014.

Žuvela-Aloise M, Koch R, Buchholz S, Früh B, 2016 Modelling the potential of green and blue infrastructure to reduce urban heat load in the city of Vienna. Clim. Chang 135, 425–438. 10.1007/s10584-016-1596-2.

HIGH LIGHTS

- We investigate the hypothetically city-level green infrastructure implementation on regional changes.
- Model showed summertime $PM_{2.5}$ increases up to 1.1 μg m^{-3} in Kansas City.
- The summertime peak O_3 decreased over the downtown areas.
- The O_3 decreases dominated by the increased NO_x titration from PBL changes
- Highlight the region-specific non-linear process feedback from green infrastructure on regional air quality

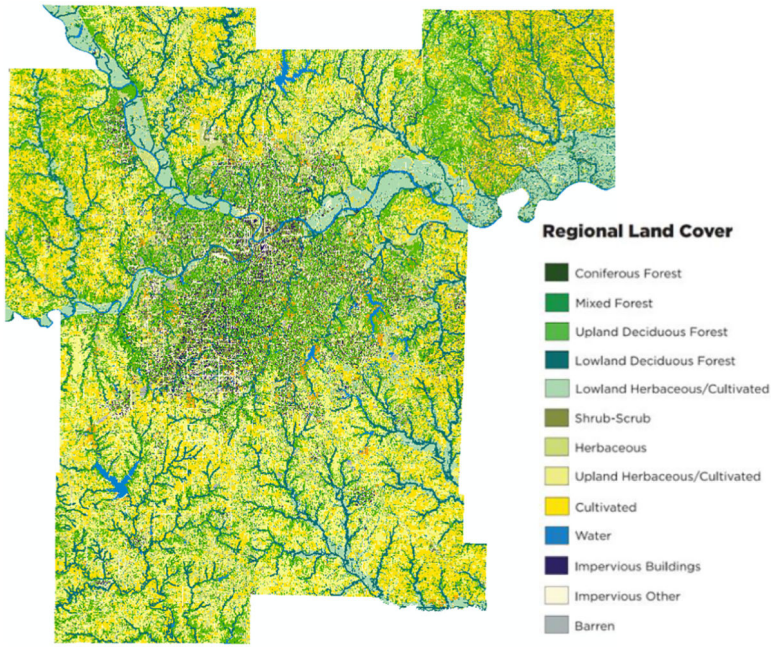

Fig. 1.

Land use maps in the greater Kansas City area for green infrastructure scenario. The differences for major land use categories can be seen in Fig. S4 in the Supporting material.

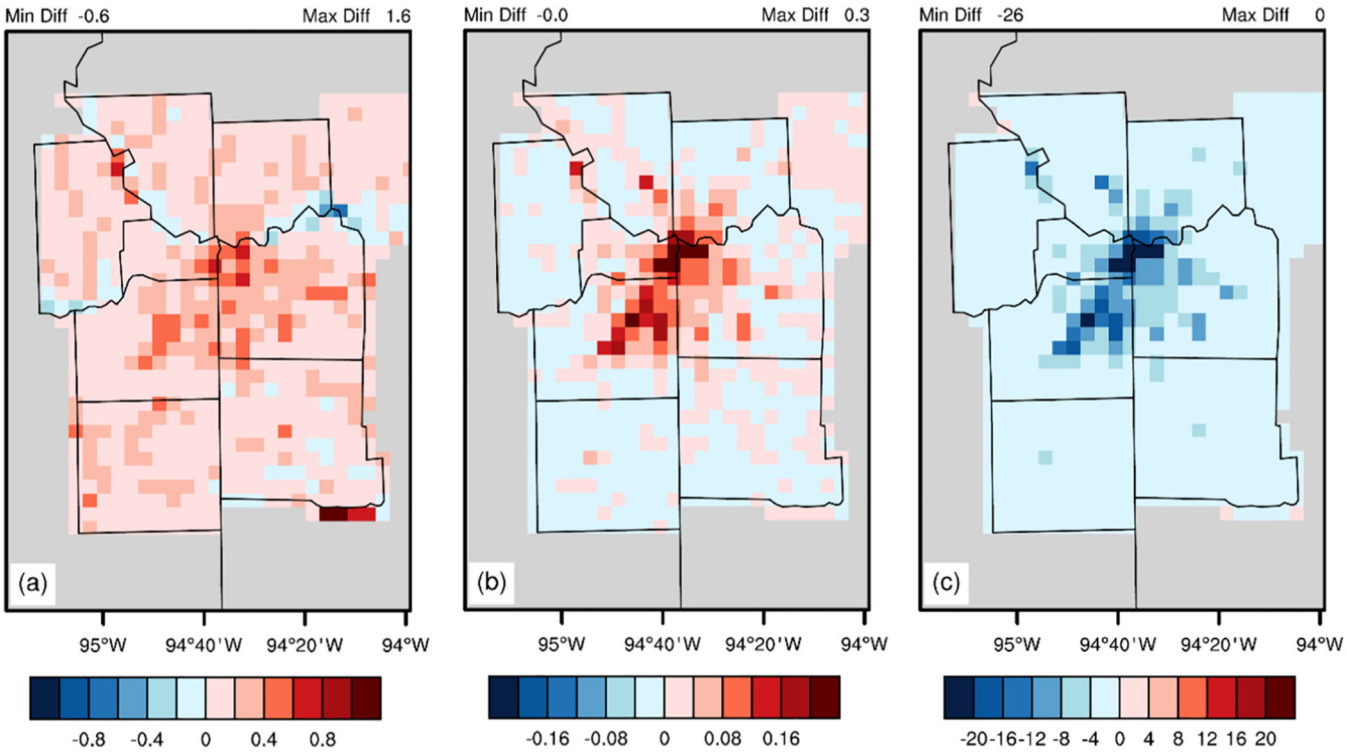

Fig. 2.

The summertime (June–July–August, JJA) changes for (a) leaf area index (LAI), (b) vegetation fraction, and (c) impervious fraction (unit %) between simulation with and without GI scenario in Kansas City. The grey areas are the regions outside Kansas City.

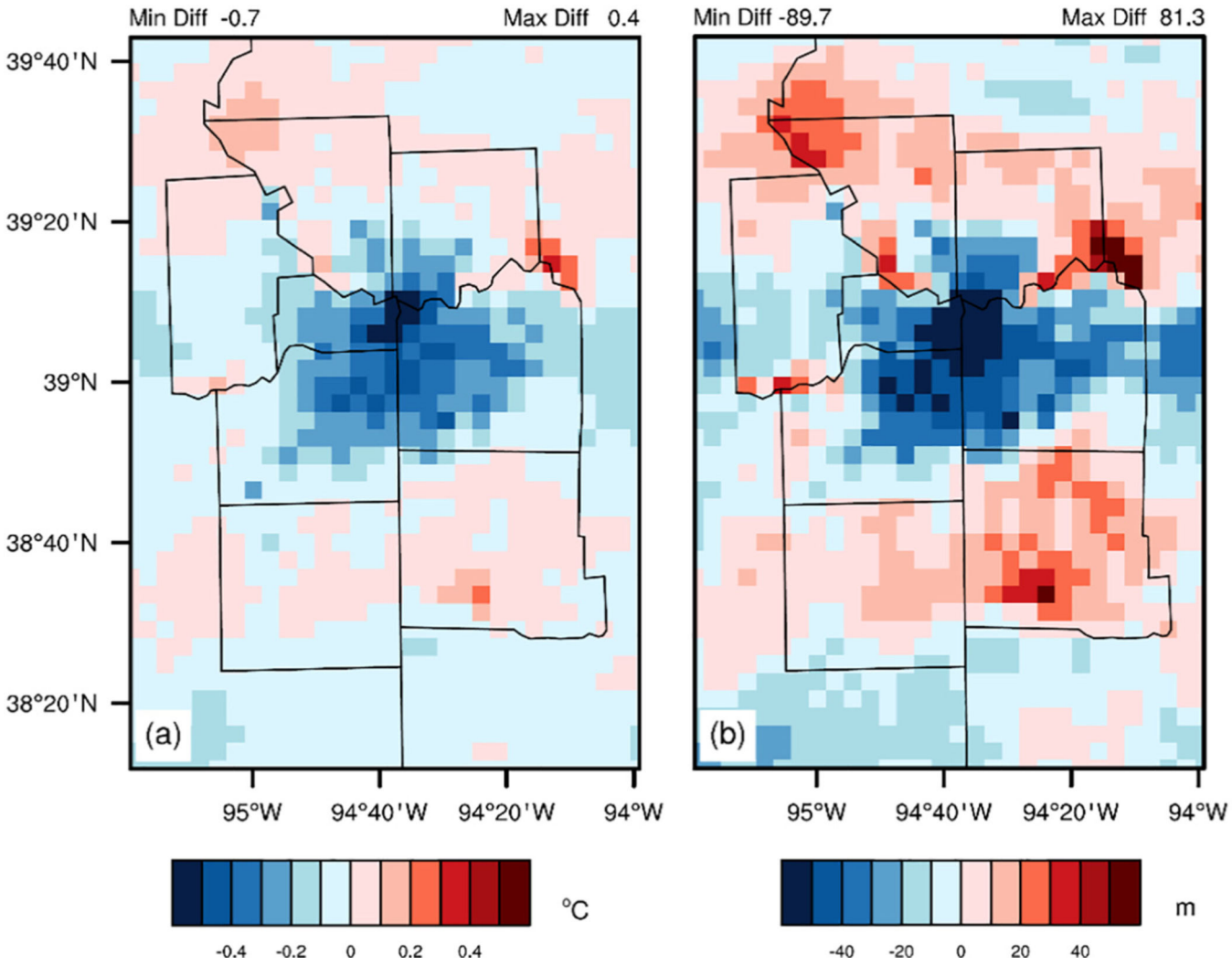

Fig. 3.

JJA mean of meteorological changes in (a) 2-m surface temperature (T2, unit of °C), and (b) planetary boundary layer height (PBLH, unit of m) after the feasible GI implementation using the WRF-Noah configuration. Also see Figs. S8 and S9 in the Supporting for the T2 and PBL changes using WRF-PX LSM scheme.

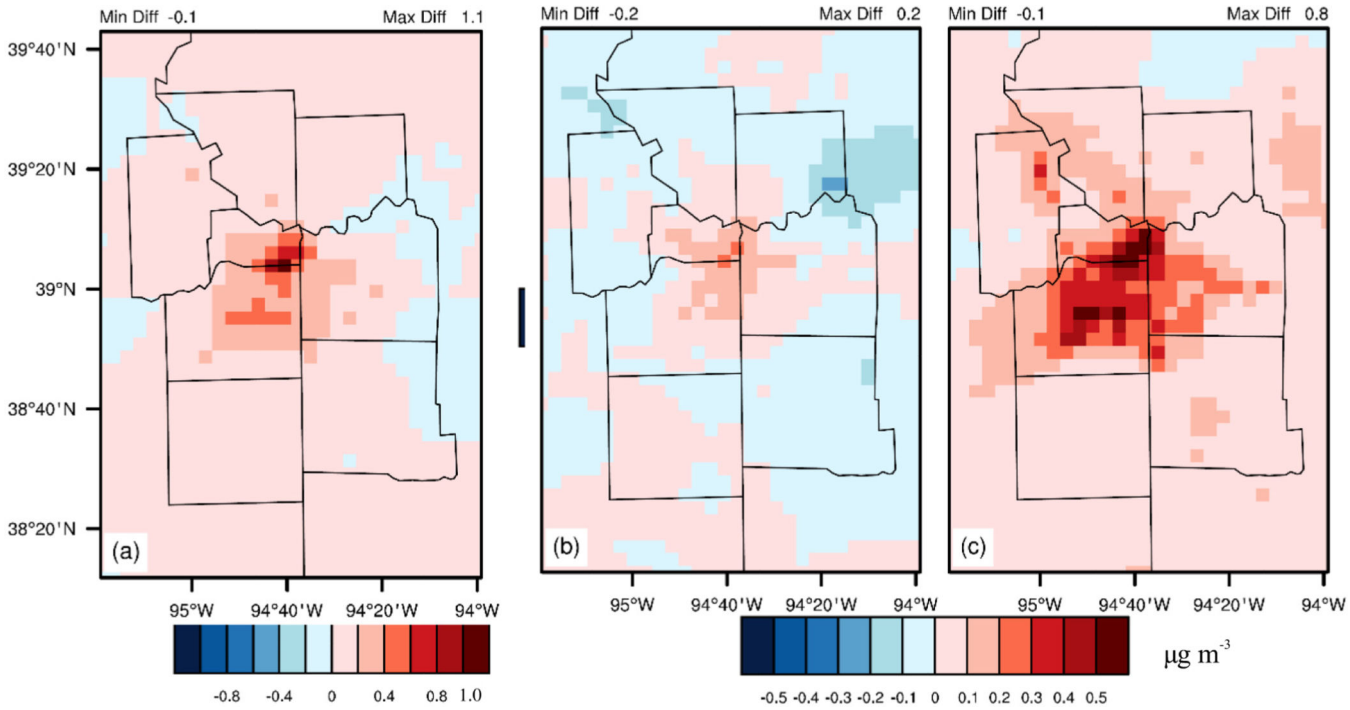

Fig. 4.

The changes in JJA of (a) 24-h average $PM_{2.5}$, (b) daytime average (Kansas City local time, 9 am-5 pm) $PM_{2.5}$, (c) nighttime average $PM_{2.5}$, between the base and the GI scenario using the WRF-Noah LSM. Unit is μg m^{-3}.

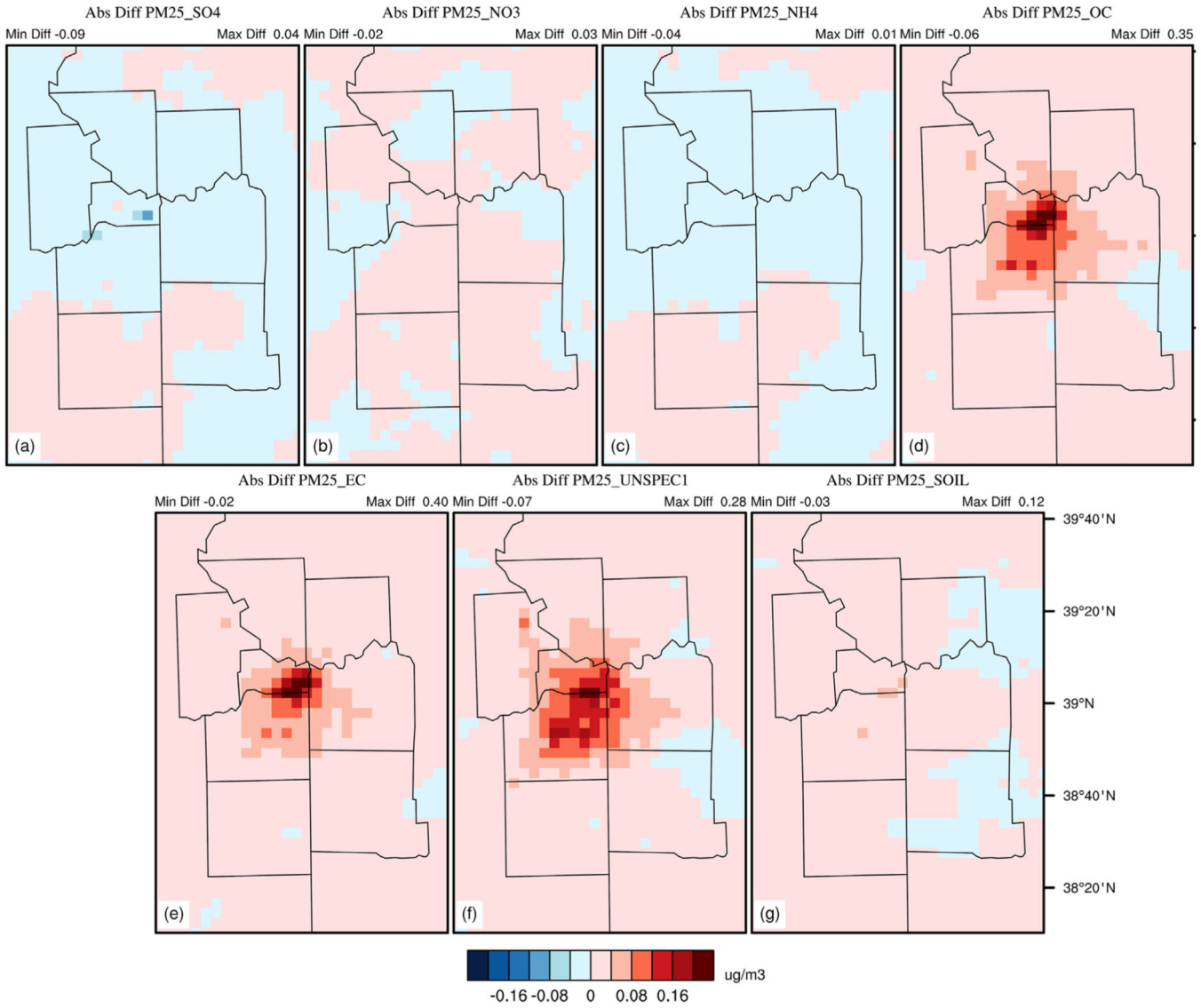

Fig. 5.

Changes between Base and GI scenarios in major $PM_{2.5}$ components for JJA: (a) sulfate (SO_4), (b) nitrate (NO_3), (c) ammonium (NH_4), (d) organic carbon (OC), (e) elementary carbon (EC), (f) unspecialized components (UNSPEC1), and (g) soil.

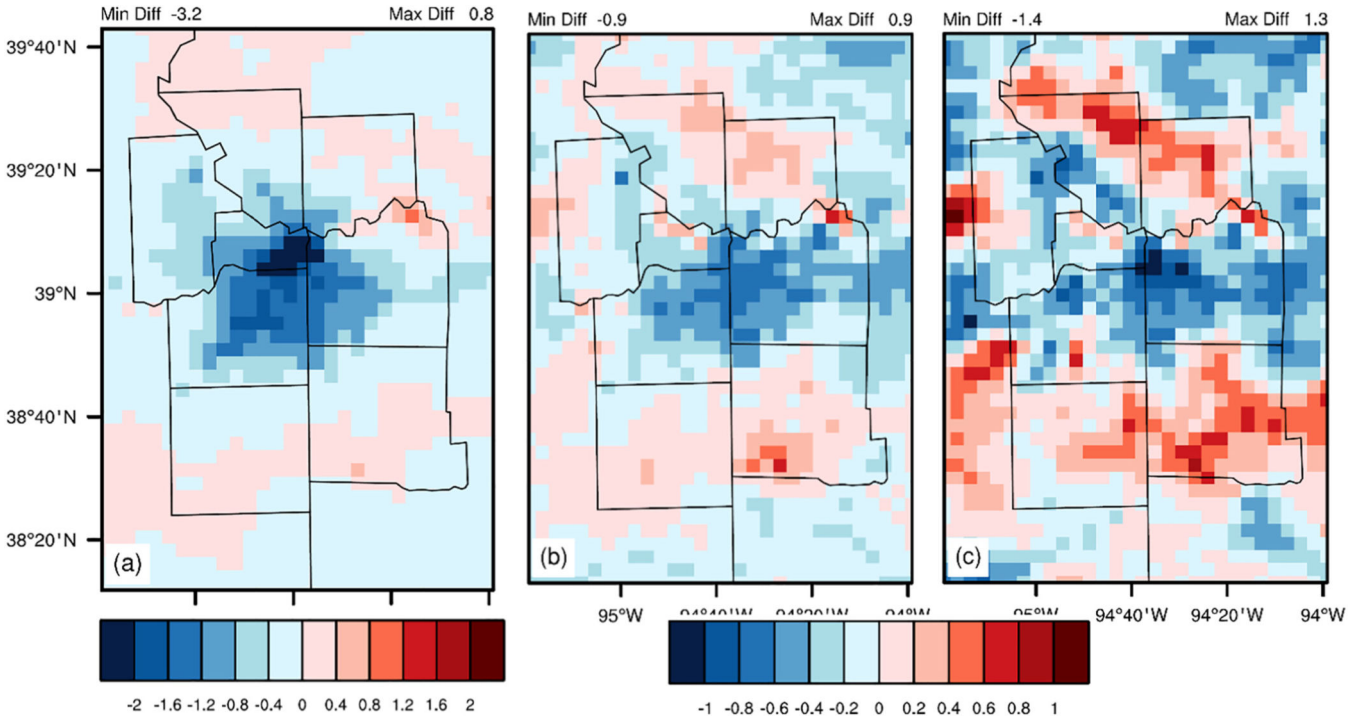

Fig. 6.

The changes in JJA mean of (a) 24-h average O_3, (b) MDA8 O_3, and (c) 1 h daily maximum O_3, after the feasible GI implementation using the WRF-Noah LSM. Unit is ppbv.

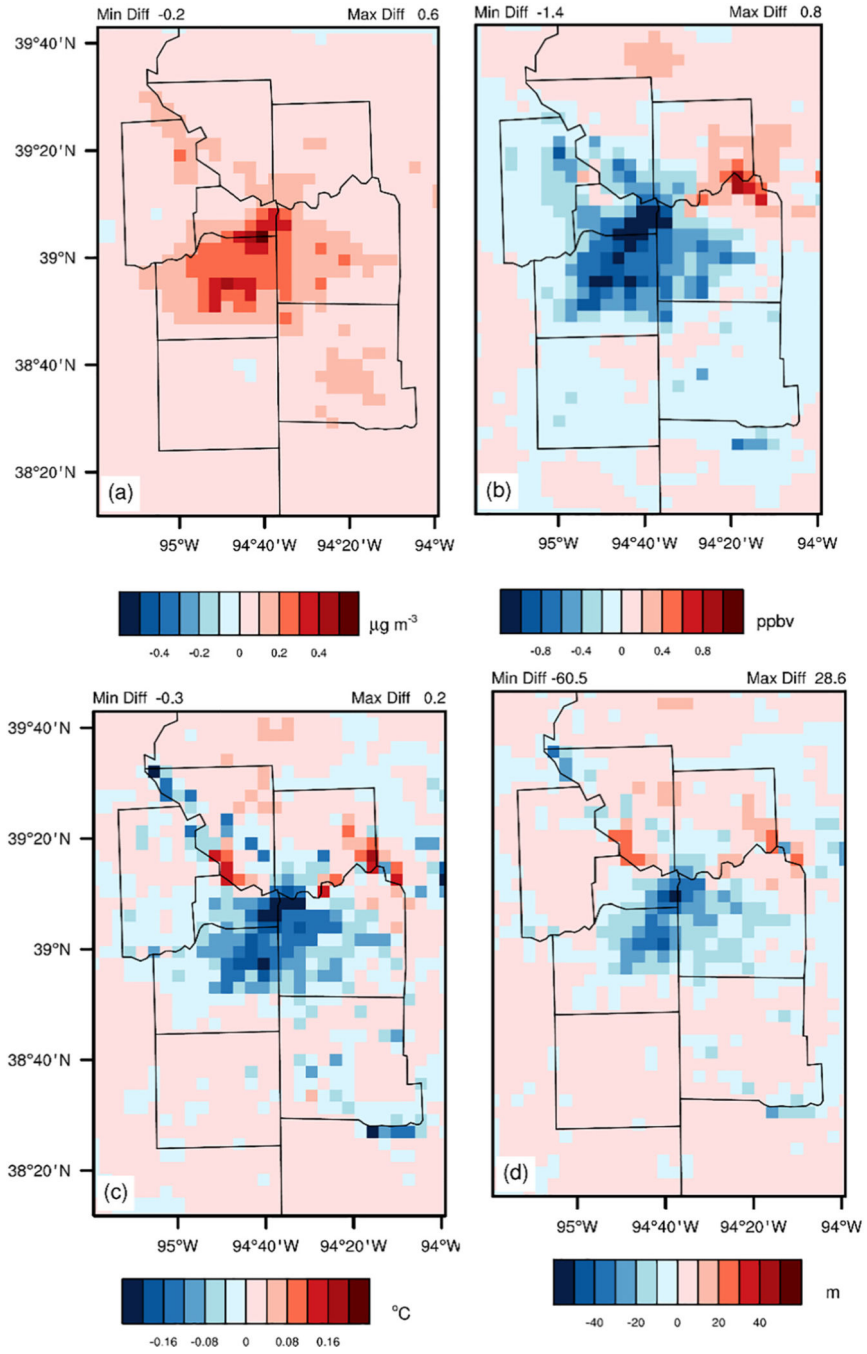

Fig. 7.

The changes of JJA average (a) 24-h $PM_{2.5}$ (μg m^{-3}), (b) 24-h O_3 (ppbv), (c) T2 (°C), and (d) PBLH (m) after the feasible GI implementation using the WRF-PX LSM.